Accepted Manuscript

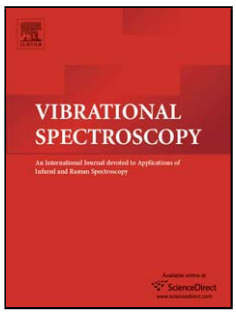

Title: Raman and Infrared Spectroscopy of $Sr_2B'UO_6$ (B' = Ni; Co) Double Perovskites

Authors: A.F.L. Moreira, A.F. García-Flores, E. Granado, N.E. Massa, R.M. Pinacca, J.C. Pedregosa, R.E. Carbonio, A. Muñoz, M.J. Martínez-Lope, J.A. Alonso, L. del Campo, D.S. Meneses, P. Echegut

PII: S0924-2031(10)00137-2
DOI: doi:10.1016/j.vibspec.2010.08.008
Reference: VIBSPE 1852

To appear in: *VIBSPE*

Received date: 22-1-2010
Revised date: 5-8-2010
Accepted date: 17-8-2010

Please cite this article as: A.F.L. Moreira, A.F. García-Flores, E. Granado, N.E. Massa, R.M. Pinacca, J.C. Pedregosa, R.E. Carbonio, A. Muñoz, M.J. Martínez-Lope, J.A. Alonso, L. del Campo, D.S. Meneses, P. Echegut, Raman and Infrared Spectroscopy of $Sr_2B'UO_6$ (B' = Ni; Co) Double Perovskites, *Vibrational Spectroscopy* (2010), doi:10.1016/j.vibspec.2010.08.008

Raman and Infrared Spectroscopy of $Sr_2B'UO_6$ (B' = Ni, Co) Double Perovskites

A. F. L. Moreira[1], A. F. García-Flores[1], E. Granado[1,2,], N.E. Massa[3], R. M. Pinacca[4], J. C. Pedregosa[4], R. E. Carbonio[5], A. Muñoz[6], M. J. Martínez-Lope [7], J. A. Alonso[7], L. del Campo[8], D. S. Meneses[8], P. Echegut[8].*

[1] Instituto de Física "Gleb Wataghin", Universidade Estadual de Campinas – UNICAMP, Caixa Postal 6165, 13083-970 Campinas, SP, Brazil

[2] Laboratório Nacional de Luz Síncrotron, Caixa Postal 6192, 13083-970, Campinas, SP, Brazil

[3] Laboratorio Nacional de Investigación y Servicios en Espectroscopía Óptica-Centro CEQUINOR- Universidad Nacional de La Plata, C.C. 962 , 1900 La Plata, Argentina

[4] Area de Química General e Inorgánica "Dr. Gabino F. Puelles", Departamento de Química, Facultad de Química, Bioquímica y Farmacia, Universidad Nacional de San Luis, 5700-San Luis, Argentina

[5] Instituto de Fisico-Quimica de Córdoba, Departamento de Físicoquímica, Facultad de Ciencias Químicas, Universidad Nacional de Córdoba, Ciudad Universitaria, 5000, Córdoba, Argentina

[6] Departamento de Física, Escuela Politécnica Superior, Universidad Carlos III de Madrid, 30 28911-Leganés, Madrid, Spain

[7] Instituto de Ciencia de Materiales de Madrid, Consejo Superior de Investigaciones Científicas, Cantoblanco, E-28049 Madrid, Spain

[8] CNRS-Conditions Extrêmes et Matériaux Haute Température et Irradiation, site Haute Température, 1D, Av. de la Recherche Scientifique, F-45071 Orléans, France

[*] *Corresponding author*
Email: egranado@ifi.unicamp.br;
PHONE (++55) 19 3521 5444;
FAX: (19) 3521 5427

Abstract

Temperature dependent normal modes and lattice thermal expansion of the $Sr_2B'UO_6$ (B' = Ni, Co) double perovskites were investigated by Raman/infrared spectroscopies and synchrotron X-ray diffraction, respectively. Monoclinic crystal structures with space group $P2_1/n$ were confirmed for both compounds, with no clear structural phase transition between 10 and 400 K. As predicted for this structure, the first-order Raman and infrared spectra show a plethora of active modes. In addition, the Raman spectra reveal an enhancement of the integrated area of an oxygen stretching mode, which is also observed in higher-order Raman modes, and an anomalous softening of ~1 cm^{-1} upon cooling below T^* ~ 300 K. In contrast, the infrared spectra show conventional temperature dependence. The band profile phonon anomalies are possibly related to an unspecified electronic property of $Sr_2B'UO_6$ (B' = Ni, Co).

Keywords: double perovskites; Raman scattering; infrared reflectivity; synchrotron X-ray powder diffraction.

1. Introduction

The general stoichiometric formula $A_2B'B''O_6$ of double perovskites is derived from the perovskite ABO_3, where the B site is occupied by two cations B' and B''. These compounds may be classified as ordered or disordered, depending on the degree of long range order of B' and B''. Ordered double perovskites typically occur when these ions show substantial charge and/or size differences. The ideal double perovskite structure has cubic symmetry with space group $Fm\bar{3}m$. However, size incompatibilities between A, B', and B'' ions with respect to the ideal structure distort the lattice, leading to a symmetry reduction to either rhombohedral, tetragonal, orthorhombic, or monoclinic unit cells. The distortions are mostly related to rotations of the $B'O_6$ and $B''O_6$ octahedra. Interest on these materials has been renewed after a large tunelling magnetoresistance was found for Sr_2FeMoO_6 and other related compounds [1-7], which was associated with half-metallic ferrimagnetic ground states. For the case of the A_2FeReO_6, novel phenomena arising from the large orbital moment of Re were also found [1, 8-12]. These discoveries illustrate the rich and still largely unexplored physics that may be found in double perovskite structures, which may be revealed as the large number of distinct possibilities for A, B' and B'' ions are further explored. In particular, as shown in the above mentioned case of B' = Fe and B'' = Re, the magnetic properties of the system may be dominated by a B'' ion which may be weakly or even non-magnetic outside the double perovskite structure.

Previous work on uranium-containing double perovskites (B' = Co, Mn, Fe, Ni, Zn; B'' = U) showed that these compounds crystallize in either partly or fully ordered monoclinic structures (space group $P2_1/n$, see Fig. 1(a)) [13,14]. Neutron powder diffraction in Sr_2CoUO_6 revealed a non-colinear magnetic arrangement of the Co moments below T_N=10 K [13], suggesting partly frustrated exchange interactions in this system. Magnetic susceptibility measurements in Sr_2NiUO_6 showed a magnetic ordering below T_N = 21 K [14]. The effective paramagnetic moments tend to deviate from the corresponding spin-only moments for B'^{2+} cations, suggesting either unquenched orbital B'^{2+} moments [13] or a partial charge disproportionation $B'^{2+} + U^{6+} <=> B'^{3+} + U^{5+}$ [14], with possible contribution of U^{5+} moments to the magnetic properties of this system. Overall, an unambiguous physical picture has not been attained for these systems yet, and further study is clearly necessary to elucidate their properties.

In the present work, we describe a lattice vibration study of $Sr_2B'UO_6$ (B' = Ni, Co) as a function of temperature, by means of Raman and infrared (IR) spectroscopies, complemented by high-resolution synchrotron X-ray powder diffraction (S-XPD) measurements of unit cell parameters. Any possible non-trivial electronic behavior for this system, such as the proposed charge disproportionation [14], should be captured by its vibrational properties. In fact, our Raman

spectra show frequency and intensity phonon anomalies at $T^* \sim 300$ K, suggesting this may be a characteristic temperature for this system. No structural transition has been observed at T^*. Our results suggest that the detected anomalies in the phonon band profiles may be electronic in origin.

2. Materials and Methods

Polycrystalline $Sr_2B'UO_6$ (B' = Ni, Co) samples were prepared by solid-state reaction, as described in Refs. [13,14]. Raman measurements were performed with a Jobin Yvon T64000 triple grating spectrometer equipped with a cryogenically cooled charge-coupled device detector. The 632.8 nm line of a He-Ne laser was used in the experiments, with power below 2 mW within a spot of ~50 μm diameter to minimize local heating. A closed cycle He cryostat was employed. Temperature dependent medium- and far-IR reflectivity spectra of polished pellets were measured between 30 cm^{-1} and 5000 cm^{-1} in a Fourier transform IR Bruker 113v with 2 cm^{-1} resolution. A gold mirror was used as 100% reference. The sample was mounted on the cold finger of a home-made cryostat for measurements between 4 K and 300 K, and the temperature was measured with a Si diode sensor mounted near the sample. High-resolution S-XPD measurements were performed in the XPD beamline of the Brazilian Synchrotron Light Laboratory (LNLS) under reflection geometry. Details of this beamline may be found in Ref. [15]. A monochromatic beam with λ = 1.3769 Å, selected by a double crystal Si(111) monochromator, was employed. A Ge(111) analyzer was used for the diffracted beam, yielding instrumental angular resolution down to ~0.01° full width at half maximum in 2θ [15]. Full diffraction profiles (10° < 2θ <150°) were measured at T = 10, 150, 300 and 400 K for B' = Co and at T = 18 and 300 K for B' = Ni. The temperature dependence of the unit cell parameters were extracted by measuring a limited but sufficient set of Bragg peaks with the powder samples mounted on the cold finger of a closed-cycle He cryostat. The parameters were refined using the GSAS+EXPGUI suite [16,17].

3. Results and Analysis

Rietveld analyses of synchrotron x-ray powder diffraction profiles confirm the fully ordered monoclinic ordered double perovskite structure with space group $P2_1/n$ previously reported for $Sr_2B'UO_6$ (B' = Ni, Co) (see Fig. 1(a)) [13,14] at all studied temperatures. Figures 1(b) and 1(c) show the temperature dependency of the refined a, b, $c'=c/(2)^{1/2}$, and β monoclinic unit cell parameters. No structural phase transition takes place in the studied temperature interval (10 K < T < 400 K) for both compounds. On warming, the monoclinic angle β shows a continuous evolution towards 90° for both materials, indicating that a transition to a more symmetric space group would

occur at very high temperatures ($T >> 400$ K), as usual for perovskite structures. It is interesting to notice that a and c' present similar temperature behavior, while b shows a significantly smaller thermal expansion. Small lattice anomalies seem to take place for B' = Co at ~60 K, which might be related to the rise of significant short-range magnetic correlations below this temperature [13].

The normal mode symmetry analysis of the double perovskite structure with space group $P2_1/n$ is summarized in Table 1. 24 Raman-active modes ($12A_g + 12B_g$) and 33 Infrared-active modes ($17A_u + 16B_u$) are expected. Figures 2(a) and 2(b) show the unpolarized first-order Raman spectra of Sr_2NiUO_6 and Sr_2CoUO_6, respectively, at selected temperatures. For Sr_2NiUO_6, 19 modes were detected at 10 K, at 110, 115, 120, 135, 145, 160, 170, 215, 245, 285, 315, 365, 375, 400, 430, 435, 485, 705, and 745 cm^{-1}. For Sr_2CoUO_6, 20 modes were observed at 12 K, at 100, 110, 115, 130, 145, 155, 170, 215, 245, 255, 285, 315, 365, 375, 380, 405, 510, 575, 650, and 735 cm^{-1}. For both compounds, the highest-energy first-order phonon at 735-745 cm^{-1} dominates the spectra with a very large relative intensity. The high frequency and large Raman cross section of this mode indicate this is the in-phase stretching vibration of the oxygen octahedra, which is Raman-active even for the cubic double perovskites [18,19]. On warming, some of the observed peaks show a large intensity decrease for Sr_2CoUO_6, which may be related to the continuous reduction of the monoclinic distortion of the unit cell (see Fig. 1(c)).

Figures 3(a-f) show the thermal evolution of the integrated intensity, frequency, and linewidth of the dominant high-energy stretching mode for Sr_2NiUO_6 and Sr_2CoUO_6. The solid lines in Figs. 3(b,c,e,f) represent the expected anharmonic behavior [20]. From these results, a characteristic temperature $T^* \sim 300$ K appears to occur in both compounds, below which the intensity of this mode increases significantly and a small but detectable softening of ~1 cm^{-1} is observed on cooling. This phonon linewidth does not present any anomalous behavior in the studied temperature interval.

Figure 4(a) shows the high-order Raman spectrum between 830 and 1165 cm^{-1} for Sr_2CoUO_6 at selected temperatures. A two-peak broad structure is observed at ~985 and 1020 cm^{-1}, for the Co-based sample only. The temperature dependence of the integrated Raman scattering in this wavenumber region is given in Fig. 4(b), after a linear background subtraction. An enhancement of this signal may be also observed on cooling below $T^* \sim 300$ K. For both samples, another two-peak structure was detected at ~1375 and 1455 cm^{-1} for B' = Co and ~1400 and 1470 cm^{-1} for B' = Ni, which intensity increases continuously under cooling (not shown). This is opposite to the conventional behavior for the Raman cross sections of higher-order phonons, which are expected to decrease on cooling due to the reduction of thermal disorder. We should mention that strong high-order phonons have been previously observed in other perovskite and double perovskite

structures, being generally ascribed to Franck-Condon excitations [21-23]. Further study is necessary to verify whether this explanation is also applicable for the compounds studied here.

The far-IR reflectivity spectrum of Sr_2CoUO_6 at 4 K is shown in Fig. 5(a). The phonon frequencies were estimated using a standard multi-oscillator dielectric fit of reflectivity spectra [24]. The dielectric function, $\varepsilon(\omega)$, is given by

$$\varepsilon(\omega) = \varepsilon_1(\omega) + i\varepsilon_2(\omega) = \varepsilon_\infty \prod_j (\Omega^2_{jLO} - \omega^2 + i\gamma_{jLO}\omega) / (\Omega^2_{jTO} - \omega^2 + i\gamma_{jTO}\omega) \qquad (1)$$

The normal reflectivity was then calculated using the Fresnel equation optimized against the experimental points, using a total of 20 oscillators. This allows estimating the high wavenumber dielectric function, $\varepsilon_{\infty;}$ the transverse and longitudinal optical frequencies, Ω_{jTO} and Ω_{jLO}, and their transverse and longitudinal damping constants, γ_{jTO} and γ_{jLO}, respectively (see Table 2). The S_j strength of the j^{th} oscillator was calculated as

$$S_j = \Omega^{-2}_{jTO} \{\prod_k \Omega^2_{kLO} - \Omega^2_{jTO}\} / \{\prod_{k\neq j} \Omega^2_{kTO} - \Omega^2_{jTO}\} \qquad , \qquad (2)$$

and are also given in Table 2.

Figures 5(b) and 5(c) show the temperature-dependence of the IR reflectivity spectrum of Sr_2CoUO_6. Under warming up to room temperature, the individual oscillator contributions in the first-order phonon region (below 800 cm^{-1}) become broader, leading to a smoothing of the far infrared phonon spectrum. In addition, a band centered at ~1400 cm^{-1} is observed, possibly arising from high-order phonon contributions. No evidence of unconventional phonon behavior was unambiguously identified in the IR data shown in Fig. 5(c).

4. Discussion

Vibrational spectroscopy, and most notably Raman scattering, has been previously identified as a powerful probe of the degree of medium-range chemical ordering in double perovskites (see, for example, ref. [25]). The large number of observed Raman and IR modes for $Sr_2B'UO_6$ (B' = Co, Ni) at low temperatures (see Figs. 2 and 5) is a clear signature of their low-symmetry ordered double perovskite structure, in agreement with x-ray diffraction data. The sharp Raman and IR vibrational features at low temperatures, associated with the low-symmetry monoclinic variant of the double perovskite structure, are somewhat smoothed upon warming. This effect appears to be more pronounced for the Raman spectra of Sr_2CoUO_6 in the spectral region below 450 cm^{-1} (see Fig. 2).

The change of behavior of the in-phase stretching mode frequency at $T^* \sim 300$ K (see Figs. 3(b,e)) may be, at first sight, explained as the result of two opposite contributions. First of all, the universal anharmonic effect tends to expand the chemical bonds and soften all phonon modes upon warming. On the other hand, the monoclinic crystal structure evolves towards a more symmetric structure on warming (see Figs. 1(b,c)). Previous ab-initio calculations on other double perovskite systems such as Ca_2AlNbO_6 indicate this mode is harder for the cubic than for the monoclinic structures [18]. Assuming this tendency may be generalized for the $Sr_2B'UO_6$ (B' = Co, Ni) systems, the evolution towards structure symmetrization at high temperatures should be accompanied by a hardening of the in-phase stretching mode, that would compete with the softening caused by anharmonicity alone. One therefore may suggest that the unusual frequency behavior shown in Figs. 3(b,e) might be a consequence of such competition. If this scenario is correct, this should be a universal behavior for oxygen stretching modes in low-symmetry perovskite structures, which might be verified for other members of this family. However, detailed studies on the temperature-dependence of stretching mode frequencies in other perovskite or double perovskite compounds are still rare in the literature. The magnetic $LaMnO_3$ [26] undoped manganite and $La_2(Co,Ni)MnO_3$ double perovskites [19,27], for instance, show frequency anomalies in their stretching vibrations below ~150-300 K, but in these cases the effect was related to magnetic ordering and ascribed to the spin-phonon coupling. Further studies on non-magnetic double perovskite systems are necessary to confirm or dismiss the universal scenario proposed here for the frequency anomalies shown in Figs. 3(b,e). We emphasize, however, that this hypothesis is not able to explain the intensity anomalies at $T^* \sim 300$ K in the Raman spectra of $Sr_2B'UO_6$ (B' = Co, Ni).

Another possible explanation for the anomalous frequency behavior reported here is the existence of a characteristic temperature $T^* \sim 300$ K for this system, that would be presumably captured by some of its vibrational degrees of freedom. This scenario is supported not only by the frequency anomaly of the symmetric stretching mode, but also by their Raman intensity behavior, which shows an enhancement below T^*. Higher-order phonons at ~1000 cm^{-1} for Sr_2CoUO_6 also shows intensity anomalies at T^*. On the other hand, no anomaly in the unit-cell parameters have been observed at T^*, ruling out a structural phase transition. Thus, in this scenario, T^* would be an electronic rather than structural characteristic temperature. Elaborating on the partial charge disproportionation scenario proposed in Ref. [14], we speculate that T^* might be related with a slight change of the equilibrium between $B'^{2+} + U^{6+} <=> B'^{3+} + U^{5+}$, which would be related with the observed intensity and frequency anomalies. Further study is necessary to confirm or dismiss this hypothesis.

5. Summary

In summary, a Raman and IR spectroscopy study was carried out on $Sr_2(Co,Ni)UO_6$. Rich vibrational spectra were observed, consistent with their monoclinic double perovskite structure. The Raman spectra show unconventional temperature dependencies for both compounds, particularly in the intensity of the first and higher order phonon modes, and in the frequency of the in-phase stretching mode. IR data on Sr_2CoUO_6, on the other hand, shows a more conventional thermal behavior. The possibility of a characteristic temperature T^*~300 K of electronic origin arises from our results, which detailed nature still remains to be elucidated.

Acknowledgments

This work was supported by Fapesp, CNPq, and CAPES, Brazil. LNLS is acknowledged for the concession of beamtime. N.E.M. acknowledges a sustenance grant by the Université d'Orléans, and partial funding from the Argentinean National Research Council (CONICET)-Project No. PIP 5152/06. J.C.P is member of CONICET.

References

[1] For a review, see D. Serrate, J.M. De Teresa, and M.R. Ibarra, J. Phys.: Condens. Matter **19**, 023201 (2007).

[2] K.-I. Kobayashi, T. Kimura, H. Sawada, K. Terakura and Y. Tokura, Nature (London) **395**, 677 (1998).

[3] K. I. Kobayashi, T. Kimura, Y. Tomioka, H. Sawada and K. Terakura. Phys. Rev. B **59** 11159 (1999).

[4] W. Prellier, V. Smolyaninova, A. Biswas, C. Galley, R.L. Greene, K. Ramesha, and J. Gopalakrishnan, J. Phys. C **12**, 965 (2000).

[5] J. Gopalakrishnan, A. Chattopadhyay, S.B. Ogale, T. Venkatesan, R.L. Greene, A.J. Millis, K. Ramesha, B. Hannoyer, and G. Marest, Phys. Rev. B **62**, 9538 (2000).

[6] A. Maignan, B. Raveau, C. Martin, and M. Hervieu, J. Solid State Chem. **144**, 224 (1999).

[7] J.M. Dai, W.H. Song, S.G. Wang, S.L. Ye, K.Y. Wang, J.J. Du, Y.P. Sun, J. Fang, J.L. Chen, and B.J. Gao, Mat. Sci. Eng. B **83**, 217 (2001).

[8] E. Granado, Q.Hung, J.W.Lynn, J.Gopalakrishnan, R.L.Greene, and K.Ramesha; Phys. Rev. B **66** , 064409 (2002)

[9] C. Azimonte, J. C. Cezar, E. Granado, Q. Huang, J. W. Lynn. J. C. P. Campoy, J. Gopalakrishnan, and K. Ramesha. Phys. Rev. Lett. **98**, 017204 (2007).

[10] C. Azimonte, E. Granado, J.C. Cezar, J. Gopalakrishnan, and K. Ramesha, J. Appl. Phys. **101**, 09H115 (2007).

[11] D. Serrate, J.M. De Teresa, P.A. Algarabel, J. Galibert, C. Ritter, J. Blasco, and M.R. Ibarra, Phys. Rev. B **75**, 165109 (2007).

[12] M. Sikora, O. Mathon, P. van der Linden, J.M. Michalik, J.M. De Teresa, Cz. Kapusta, and S. Pascarelli, Phys. Rev. B **79**, 220402 (2009).

[13] R. M. Pinacca, M. C. Viola, J. C. Pedregosa, A. Muñoz, J. A. Alonso, M.J. Martínez-Lope, R. E. Carbonio. Dalton Trans. **447**, (2005).

[14] R. M. Pinacca, M. C. Viola, J. C. Pedregosa, M. J. Martínez-Lope, R. E. Carbonio, J. A. Alonso. J. Sol. State Chem. **180**, 1582 (2007).

[15] F. F. Ferreira, E. Granado, W. Carvalho Jr., S.W. Kycia, D. Bruno, R. Droppa Jr. J. Synchrotron Rad. **13**, 46 (2006).

[16] A.C. Larson and R.B. Von Dreele, Los Alamos National Laboratory Report LAUR 86-748 (2000).

[17] B. H. Toby, J. Appl. Cryst. **34**, 210-213 (2001).

[18] S.A. Prosandeev, U. Waghmare, I. Levin, and J. Maslar, Phys. Rev. B **71**, 214307 (2005).

[19] M.N. Iliev, M.V. Abrashev, A.P. Litvinchuk, V.G. Hadjiev, H. Guo, and A. Gupta, Phys. Rev. B **75**, 104118 (2007).

[20] M. Balkanski, R. F. Wallis, and E. Haro. Phys. Rev. B **28**, 1928 (1983).

[21] J. Andreasson, J. Holmlund, C.S. Knee, M. Käll, L. Börjesson, S. Naler, J. Bäckström, M. Rübhausen, A.Z. Azad, and S.-G. Eriksson, Phys. Rev. B **75**, 104302 (2007).

[22] Y. Fujioka, J. Frantti, and M. Kakihana, J. Phys. Chem. B **108**, 17012 (2004).

[23] Y. Fujioka, J. Frantti, and M. Kakihana, J. Phys. Chem. B **110**, 777 (2006).

[24] T. Kurosawa, J. Phys. Soc. Jpn **16**, 1208 (1961).

[25] I.G. Siny, R.S. Katiyar, and A.S. Bhalla, Ferroelectr. Rev. **2**, 51 (2000).

[26] E. Granado, A. García, J.A. Sanjurjo, C. Rettori, I. Torriani, F. Prado, R.D. Sánchez, A. Caneiro, and S.B. Oseroff, Phys. Rev. B **60**, 11879 (1999).

[27] M.N. Iliev, H. Guo, and A. Gupta, Appl. Phys. Lett. **90**, 151914 (2007).

FIGURE CAPTIONS

Figure 1: (a) Crystal structure of Sr_2CoUO_6. Temperature dependence of the unit cell parameters of $Sr_2B'UO_6$ for (b) B'=Ni, and (c) B'=Co.

Figure 2: Unpolarized Raman spectra of (a) Sr_2NiUO_6 and (b) Sr_2CoUO_6 at selected temperatures.

Figure 3: Temperature dependence of (a,d) integrated intensity, (b,e) frequency, and (c,f) linewidth of the Raman-active in-phase oxygen stretching mode for (a-c) Sr_2NiUO_6 and (d-f) Sr_2CoUO_6.

Figure 4: (a) Selected portion of the Raman spectra of Sr_2CoUO_6 in the high-energy higher-order phonon region for selected temperatures. (b) Temperature dependence of the integrated area of the scattering in the spectral region displayed in (a), after a linear background subtraction.

Figure 5: (a) Far infrared near normal reflectivity of Sr_2CoUO_6 at 4K; circle: experimental data, full line: multi-oscillator dielectric fit (see text); (b) temperature dependent mid-infrared near normal reflectivity (weak features centered at ~1370 cm^{-1} are assigned to vibrational overtones); (c) temperature dependent far-infrared near normal reflectivity. The spectra in panels (b) and (c) were vertically displaced for clarity.

Table 1. Normal mode symmetry analysis for the monoclinic structure of $Sr_2B'UO_6$ (B' = Co, Ni) (space group $P2_1/n$).

Atoms	Wyckoff notation	Site Symmetry	Irreducible Representation
Sr^{2+}	4e	C_1	$3A_g + 3A_u + 3B_g + 3B_u$
B'^{2+}	2b	C_i	$3A_u + 3B_u$
U^{6+}	2d	C_i	$3A_u + 3B_u$
O1	4e	C_1	$3A_g + 3A_u + 3B_g + 3B_u$
O2	4e	C_1	$3A_g + 3A_u + 3B_g + 3B_u$
O3	4e	C_1	$3A_g + 3A_u + 3B_g + 3B_u$
			$\Gamma_{Cristal} = 12A_g + 18A_u + 12B_g + 18B_u$
		Normal mode classification	
			$\Gamma_{Raman} = 12A_g$ (xx, yy, zz, xy) + $12B_g$ (xz,yz)
			$\Gamma_{IR} = 17A_u + 16B_u$
			$\Gamma_{Acoustic} = A_u + 2B_u$

Table 2. Dielectric simulation fitting parameters for Sr_2CoUO_6 at 4 K.

T (K)	ε_∞	Ω_{to} (cm^{-1})	Ω_{lo} (cm^{-1})	γ_{to} (cm^{-1})	γ_{lo} (cm^{-1})	S_j
4 K	2.33	71.5	72.2	32.9	26.8	0.38
		76.3	76.5	0.5	0.6	0.04
		83.6	84.2	3.3	3.4	0.31
		101.3	123.4	103.9	112.5	5.30
		131.4	132.1	10.2	3.3	0.20
		133.4	140.5	6.0	13.3	0.31
		149.8	159.0	9.1	5.1	0.39
		181.2	186.3	193.9	221.1	0.27
		187.0	187.6	7.1	7.9	0.005
		214.0	227.1	17.8	7.0	0.71
		239.6	242.2	18.1	18.6	0.10
		258.3	271.2	17.3	17.0	0.50
		284.5	294.4	11.3	25.0	0.26
		306.4	316.0	21.0	26.5	0.22
		321.2	325.1	8.7	21.4	0.02
		339.2	350.9	15.0	21.0	0.15
		372.2	380.3	31.8	11.4	0.14
		400.2	438.0	747.6	1224.7	0.27
		553.6	623.4	62.7	189.3	0.39
		668.0	682.4	212.3	20.5	0.01

Figure 1

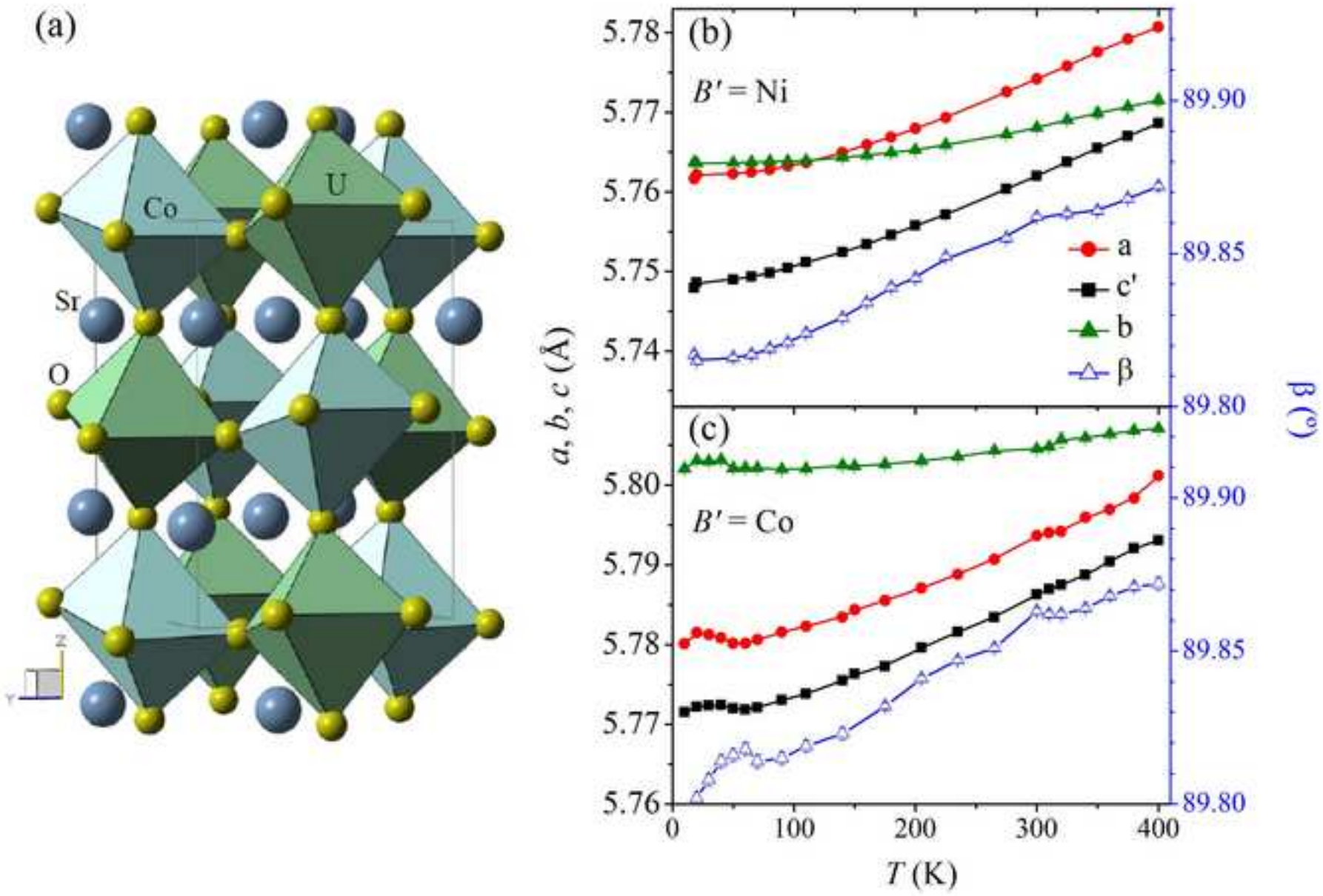
(a)
Co
U
Sr
O
(b)
B′ = Ni
(c)
B′ = Co
a
c'
b
β
a, b, c (Å)
β (°)
T (K)
5.78
5.77
5.76
5.75
5.74
5.80
5.79
5.78
5.77
5.76
89.90
89.85
89.80
0
100
200
300
400

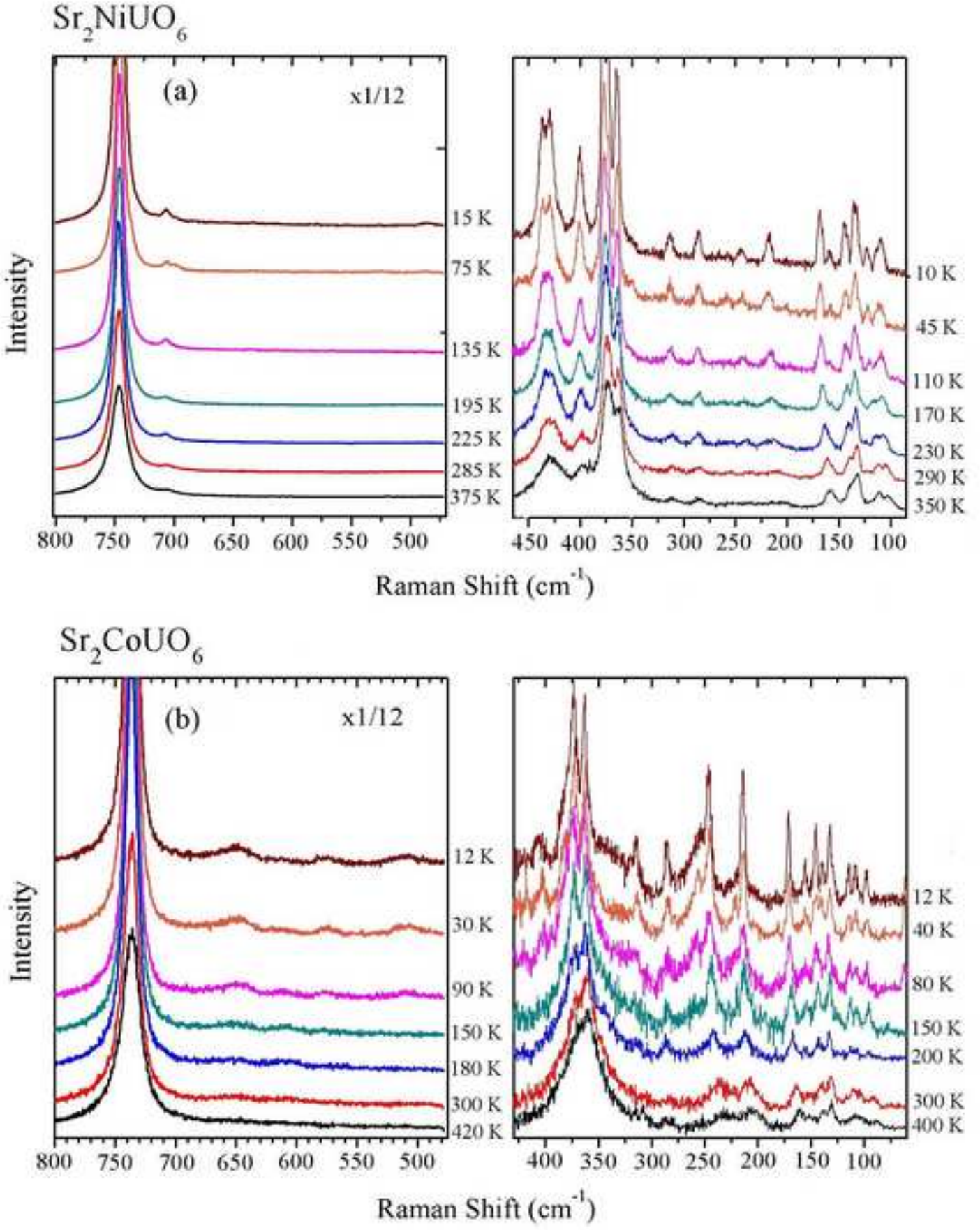

Figure 3

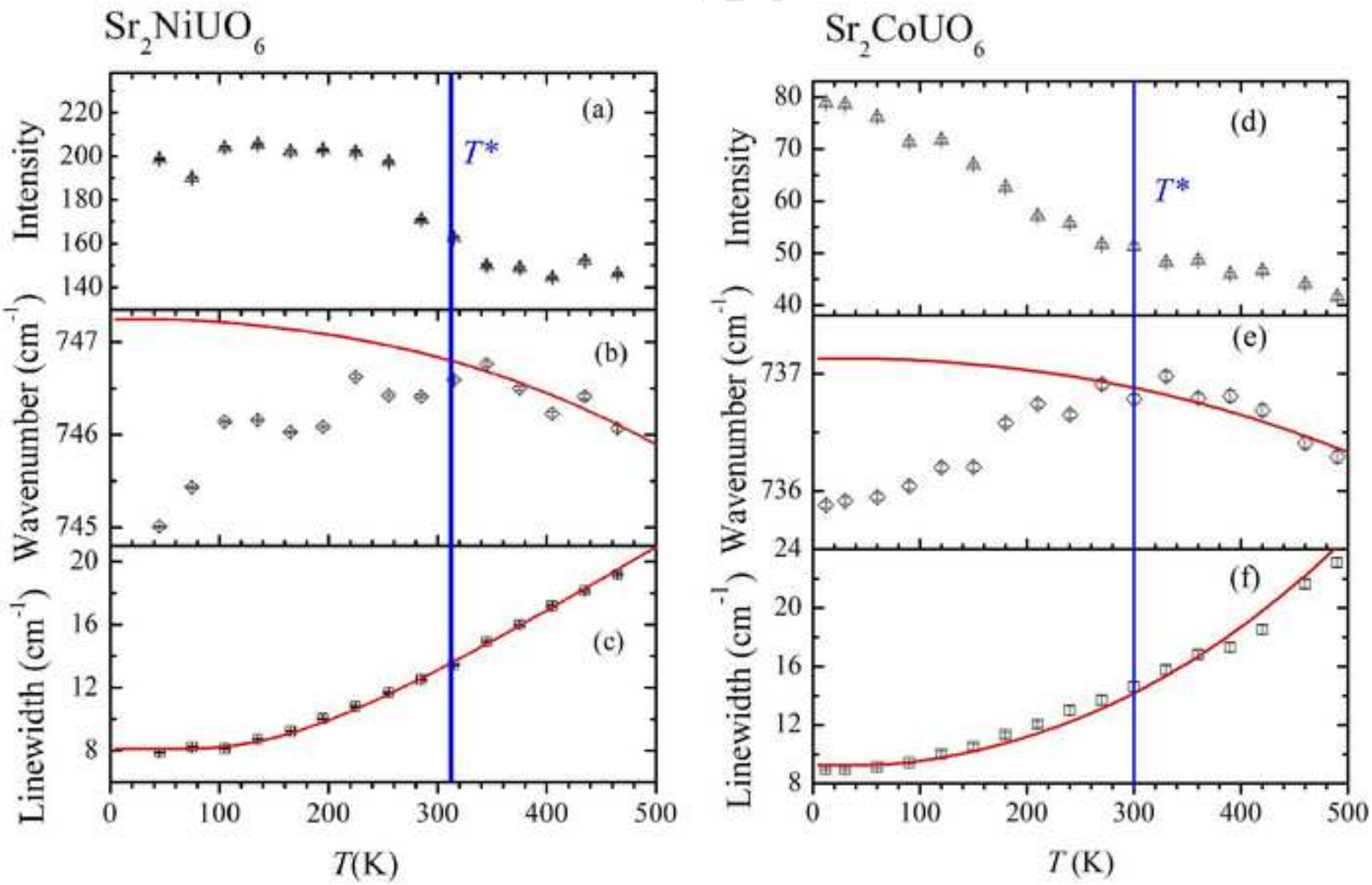
Sr2NiUO6
Sr2CoUO6
Intensity
Wavenumber (cm-1)
Linewidth (cm-1)
T*
(a)
(b)
(c)
(d)
(e)
(f)
T(K)
T (K)

Figure 4

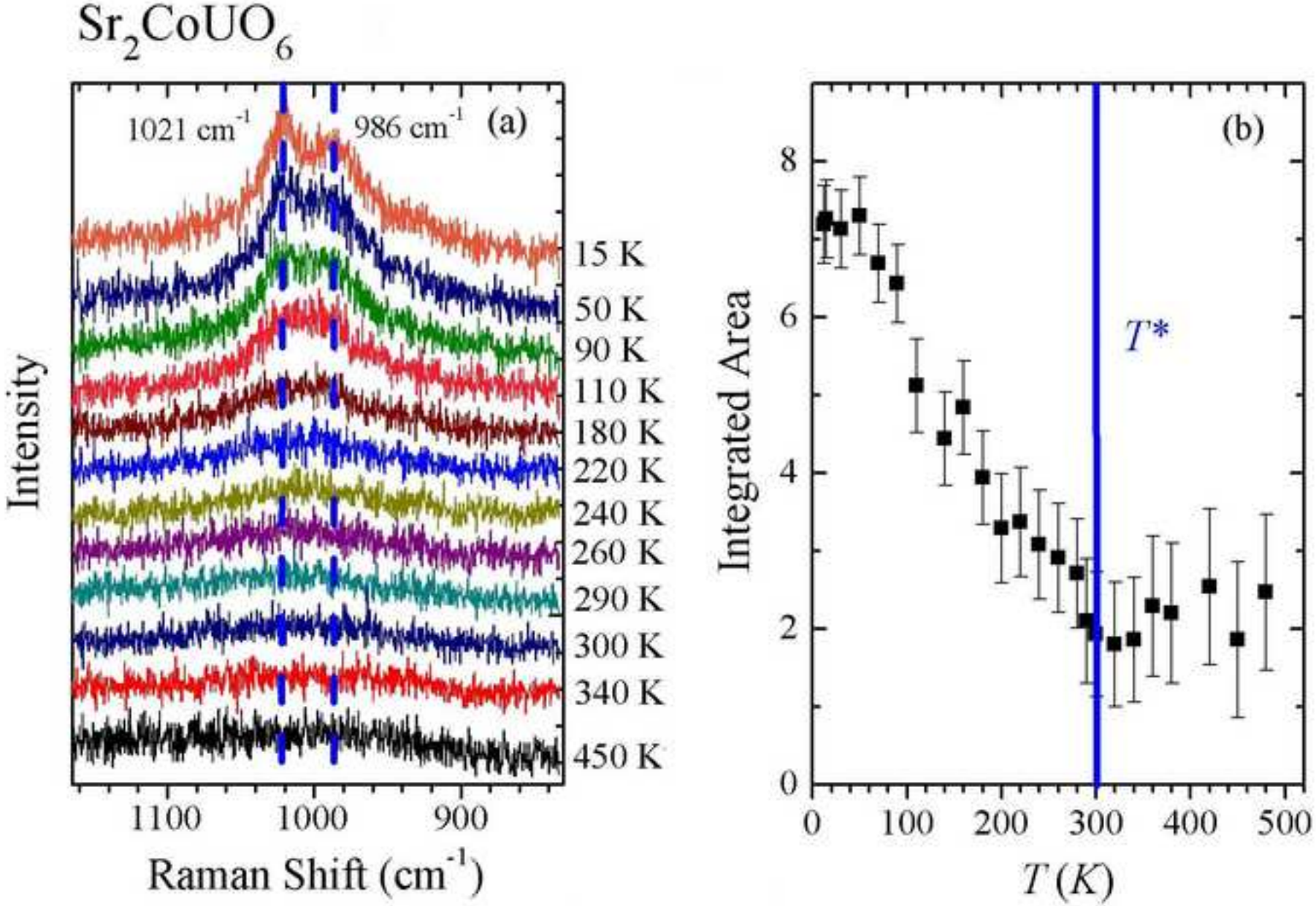
Sr2CoUO6
1021 cm-1
986 cm-1
(a)
15 K
50 K
90 K
110 K
180 K
220 K
240 K
260 K
290 K
300 K
340 K
450 K
Intensity
1100
1000
900
Raman Shift (cm-1)
(b)
T*
Integrated Area
0
2
4
6
8
0
100
200
300
400
500
T (K)